

Short communication

Fabrication and characterization of components for cube shaped micro tubular SOFC bundle

Yoshihiro Funahashi^{a,*}, Toru Shimamori^b, Toshio Suzuki^c,
Yoshinobu Fujishiro^c, Masanobu Awano^c

^a *Fine Ceramics Research Association (FCRA), 2266-99 Anagahora, Shimo-shidami, Moriyama-ku, Nagoya 463-8561, Japan*

^b *NGK Spark Plug Co., Ltd., Japan*

^c *National Institute of Advanced Industrial Science and Technology (AIST), Japan*

Received 7 August 2006; received in revised form 2 October 2006; accepted 3 October 2006

Available online 9 November 2006

Abstract

Solid oxide fuel cells (SOFCs) have the highest energy efficiency among various power generators. However, SOFCs generally have problems regarding to heat stress due to the heating cycle during cell operation, especially quick start-up/shut-down and the size of SOFC systems, which limit their application use. Micro tubular SOFCs are expected to be a solution to these problems because they are considered to be robust for repeated cycling under rapid changes in cell operating temperatures. If highly dense micro tubular SOFC stacks become available, it will accelerate development of SOFC systems, as well as increase a variety of applications. Our study aims to fabricate compact and high power SOFC bundles, which are composed of tubular SOFCs with the diameter of sub-millimeters. In this study, as the first stage of the development, processing technologies of tubular SOFCs and cube shaped cathode matrices were examined. Micro tubular SOFCs were fabricated using extrusion and co-firing techniques. The tubular SOFCs were then, arranged in the cathode matrices, which were piled up to be a cube shaped bundle. Each component of the cube shaped micro tubular SOFC bundle (cube) will be discussed in detail.

© 2006 Elsevier B.V. All rights reserved.

Keywords: SOFC; Micro tubular; Fabrication; Modeling; Microstructure

1. Introduction

SOFCs are known as high efficiency energy sources among other type of fuel cells because SOFC systems can utilize waste heat from high temperature operation. SOFCs are essentially not suffering from severe problems that PEFCs currently confront. For example, PEFCs are easily poisoned by carbon monoxide in the reforming gas [1], and moisture in the fuel gas needs to be exactly managed during operation [2]. SOFCs can also offer direct hydrocarbon injection, which is beneficial for practical application [3].

So far, SOFC systems were mainly designed and developed as stationary generator units [4] due to high temperature operation

and the use of ceramic components. In Addition, SOFC systems tended to be larger and needed many auxiliaries such as heating unit, a high heat-insulating package. Therefore, they could not bear to be operated in quick start-up/shut-down [5] neither be applied to portable use.

Currently, many studies on SOFCs have been reported that application fields of SOFC spread out, by downsizing of SOFCs [6–9] and/or lowering SOFC operating temperature [10–12]. It was shown that small-scale tubular SOFCs endured thermal stress caused by rapid heating up to operating temperature. Use of small-scale tubular SOFCs enables to design cell stacks with high volumetric power density due to increased electrode area in volume, which leads to lowering operating temperature to achieve the same cell performance.

The purpose of this research is to develop fabrication technology for integrating micro tubular SOFCs of 0.5–2.0 mm in diameter to produce cube shaped cell bundles. In this paper, each component of the cubes will be presented and discussed in detail.

* Corresponding author. Tel.: +81 52 736 7665; fax: +81 52 736 7665.

E-mail addresses: y-funahashi@aist.go.jp (Y. Funahashi),
t-shimamori@mg.ngkntk.co.jp (T. Shimamori), toshio.suzuki@aist.go.jp
(T. Suzuki), y-fujishiro@aist.go.jp (Y. Fujishiro), masa-awano@aist.go.jp
(M. Awano).

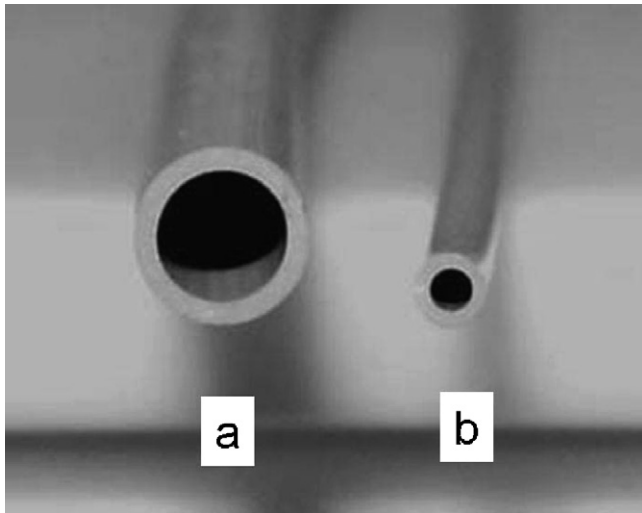


Fig. 1. The appearance of extruded green tubes: (a) outside 2.4 mm, inside 1.8 mm; (b) outside 1.0 mm, inside 0.6 mm.

2. Experimental

2.1. Micro tubular cells

Anode tubes were made from NiO powder (Seimi Chemical Co., Ltd.), $\text{Gd}_{0.2}\text{Ce}_{0.8}\text{O}_{2-x}$ (GDC) (Shin-Etsu Chemical Co., Ltd.), poly methyl methacrylate beads (PMMA) of 5 μm in diameter (Sekisui Plastics Co., Ltd.), and cellulose (Yuken Kogyo Co., Ltd.). These powders were mixed for 1 h by a mixer 5DMV-rr (Dalton Co., Ltd.), and after adding the proper amount of water; it was stirred for 30 min in a vacuumed chamber. The mixture (clay) that was prepared from these powders was left over 15 h for aging. The tubes were extruded from a metal mold by using a piston cylinder type extruder (Ishikawa-Teki Tekko-sho Co., Ltd.). Fig. 1 shows the appearance of extruded tubes after drying. The diameters of the tubes were 2.4 and 1.0 mm, respectively.

A slurry for dip-coating electrolyte was prepared by mixing the GDC powder, solvents (methyl ethyl ketone and ethanol), binder (poly vinyl butyral), dispersant (polymer of an amine system) and plasticizer (dioctyl phthalate) for 24 h. The anode green tubes were dipped in the slurry and coated at the pulling rate of 1.5 mm s^{-1} . The coated films were dried in air. The anode green tubes coated with the slurry were co-sintered at 1400°C for 1 h in air. The anode tubes with the electrolyte layer were, again,

dip-coated using cathode slurry, which was prepared in the same manner using $\text{La}_{0.6}\text{Sr}_{0.4}\text{Co}_{0.2}\text{Fe}_{0.8}\text{O}_{3-y}$ (LSCF) (Seimi Chemical, Co., Ltd.), the GDC powder, and organic ingredients. After dip-coated, the tubes were dried and sintered at 1000°C for 1 h in air. The cell size of the completed cells are 2.0 and 0.8 mm in diameter respectively, with 15–50 mm in length (cathode length of 6–30 mm).

The microstructure of the tubular cells was observed by using SEM (JEOL, JSM6330F). The shrinkage of the anode tubes at the sintering process was investigated with TMA8310 (Rigaku Co., Ltd.), and the porosity of the anode tubes was measured by using mercury porosimeter (CE instruments Co., Ltd., Pascal 440). The cell performance was investigated by using a potentiostat (Solartron 1296). The cell size used for single cell measurement was 2.0 mm in diameter and 15 mm in length with cathode length of 6 mm, whose effective cell area was 0.38 cm^2 . The Ag wire was used for collecting current from anode and cathode sides, which were both fixed by Ag paste. The current collection from anode side was made from an edge of the anode tube, and the collection from cathode side was made from whole cathode area. Hydrogen (humidified by bubbling water at room temperature) was flowed inside of the tubular cell at the rate of 25 mL min^{-1} . The cathode side was open to the air without flowing gas.

2.2. Cathode matrices for cube shaped micro tubular SOFC bundles

Cathode matrices with several grooves which hold the micro tubular SOFCs were designed to build cube shaped micro tubular SOFC bundles. The cathode matrices have following roles: (i) current collectors (ii) guides for cell arrangement and (iii) gas (air) flow paths. The cathode matrices were made from LSCF powder (Daiichi Kigenso Kagaku Kogyo Co., Ltd.) and cellulose (Yuken Kogyo Co., Ltd.). They were mixed using the same steps as the anode preparation. In order to satisfy the requirements of cathode matrices as described above, 20 μm particle size of LSCF powder was selected. The matrices were prepared by extruding the clay from a metal mold using a screw cylinder type extruder (Miyazaki Tekko Co., Ltd.). The extruded matrices were cut to 3 cm long, dried and sintered in air. The shape of the cathode matrix was 3 cm wide, 3 cm long and 6 mm thick, with 6 grooves whose width were 2.3 mm on both the $3 \text{ cm} \times 3 \text{ cm}$ surfaces.

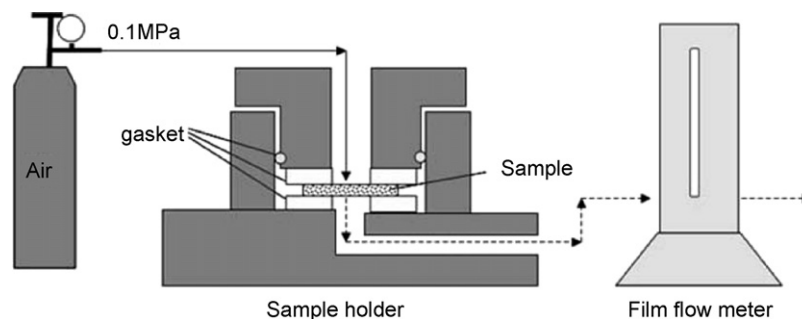


Fig. 2. The experimental apparatus for measuring gas penetration.

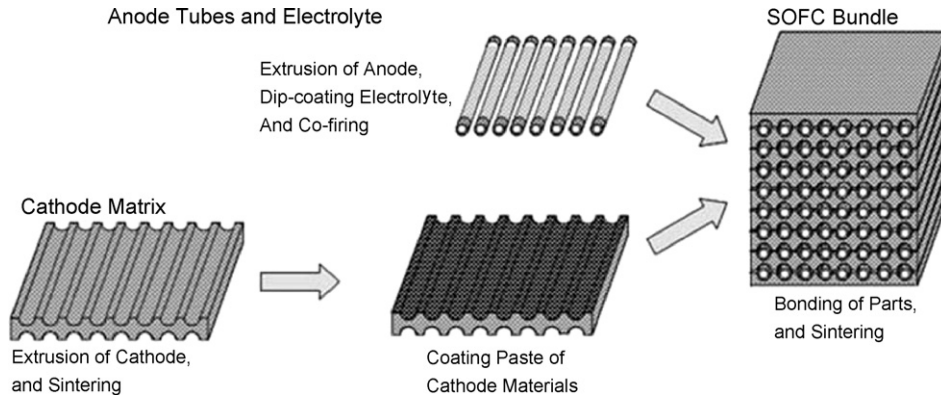


Fig. 3. The procedure of assembling cube shaped micro tubular SOFC bundles.

The gas penetration test of the cathode matrices was conducted using the experimental apparatus shown in Fig. 2. The gas pressure was applied to one side of the sample, and the amount of penetrated gas was measured using a soap film flow meter. The cathode matrix without the grooves was used for this measurement, which turned out to be a foursquare plate of 2.5 mm thick.

2.3. Assembly of cube shaped micro tubular SOFC bundles

Fig. 3 shows the procedure of assembling cube shaped micro tubular SOFC bundles. A bonding paste for assembling the cubes was prepared by mixing LSCF powder (Seimi chemical Co., Ltd.), the binder (cellulose), the dispersant (polymer of an amine system), and the solvent (diethylene glycol monobutyl ether). The paste was screen-printed on the surface of the cathode matrices, followed by the placement of 5 cm long tubular cells with cathode length of 3 cm, before the paste was dried. After the cube was assembled by sandwiching the cathode matrices and the tubular cells, the cube was sintered at 1000 °C for 1 h in air. Since the paste was prepared from cathode materials, it can utilize as the two-layered cathode structures.

3. Results and discussion

3.1. Micro tubular cells

It is important to improve the gas diffusion in the anode in order to increase cell performance. Thus, an attempt was made to control anode structure by adding pore former without impairing gas tightness of the electrolyte during the co-sintering process.

Fig. 4 shows anode shrinkage as a function of sintering temperature. As can be seen, when the PMMA beads were used as the pore former, the sintering behavior of the tubular cell did not change from that without the pore former, and even did not change with an amount of PMMA. As a comparison, Fig. 4 also shows the result of the sintering behavior for a sample added carbon powder as a pore former, which showed different behavior. This behavior may be caused by the fact that the carbon powder was pretty bulkier than PMMA beads, which leads to the difference in the packing density of the powder.

Fig. 5(a–d) shows the microstructure of the samples added different amount of PMMA beads, 10, 20, 30, and 40 vol.% PMMA in the clay, respectively. It was shown that the porosity of the anode tubes can be controlled by the amount of the PMMA beads. Especially the sample added 40 vol.% PMMA had a lot of connective path for gas diffusion.

Fig. 6 shows the distribution of the pore diameter in the anode tubes that was measured by a mercury porosimeter. The main peak of the pore diameter distribution shifted from 0.6 to 1 μm as the amount of PMMA increased. These results were consistent with the SEM observation as shown in Fig. 5. The porosity of the anode which were added 0, 10, 20, 30, and 40 vol.% PMMA were 36, 39, 41, 47, and 51%, respectively, after reduction.

Fig. 7 shows the SEM cross-section images of 10 and 40 vol.% PMMA added samples with co-sintered electrolyte. As can be seen, dense electrolyte with 10 μm thick was successfully prepared on the porous anode tube using slurry coating and co-sintering technique developed in this study. These results showed that using PMMA as the pore former can control anode microstructure without impairing gas tightness of the electrolyte, since it was shown that the amount of PMMA did not affect on the shrinkage of the anode tube during sintering.

Fig. 8 shows the result of fuel cell tests for tubular cells with different anode porosity controlled by changing the amount of PMMA. As can be seen, the maximum output power density at 550 °C was improved from 0.28 to 0.46 W cm⁻² when the

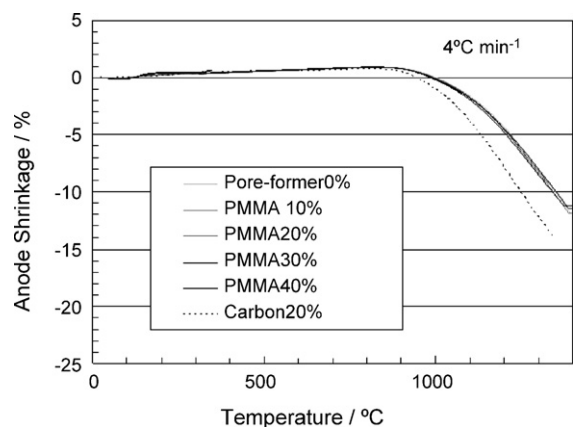


Fig. 4. Anode shrinkages as a function of sintering temperature.

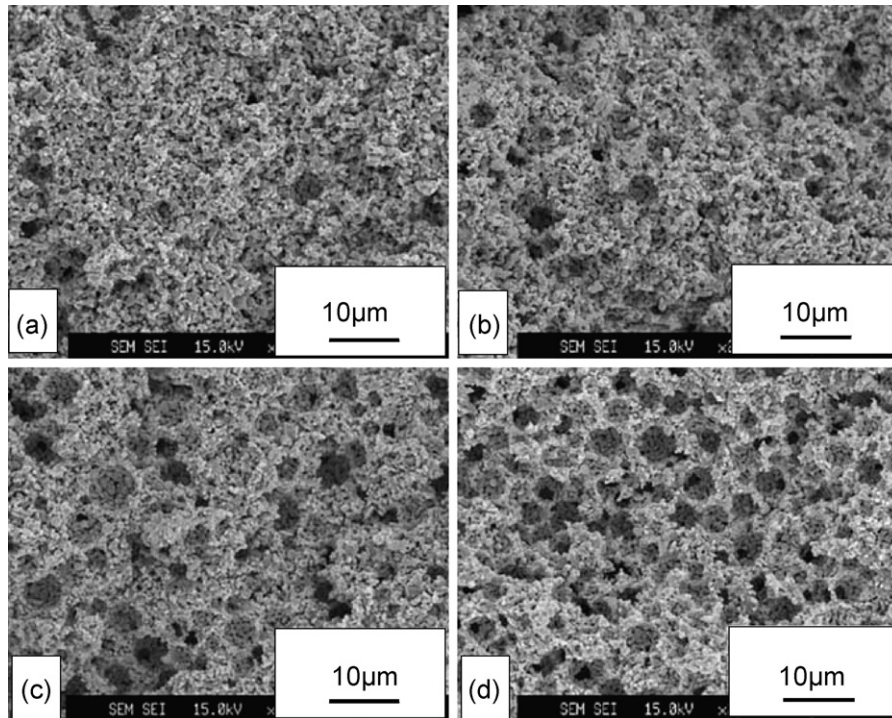


Fig. 5. Microstructure of the anode tubes after reduction: (a) PMMA 10 vol.%; (b) PMMA 20 vol.%; (c) PMMA 30 vol.%; (d) PMMA 40 vol.%.

amount of PMMA increased from 20 to 40 vol.%. Thus, the gas diffusion in the anode tube is thought to be important point to improve the performance of the cell.

3.2. Cathode matrices for cube shaped micro tubular SOFC bundles

The gas penetrability in the cathode matrices is thought to be a key factor to improve the performance of the cube. Table 1 shows

the gas penetration coefficients of the cathode matrices prepared using 20 μm LSCF powder for each calcination temperature, determined from following equation,

$$C_g = \frac{FT}{60AP} \quad (1)$$

where C_g , F , T , A and P are gas penetration coefficient, gas flow rate (mL min^{-1}), thickness of sample (cm), area of gas penetration (cm^2) and pressure difference (Pa), respectively. It was shown that the gas penetration coefficients changed from 1.68×10^{-4} to $1.35 \times 10^{-4} \text{ mL cm cm}^{-2} \text{ s}^{-1} \text{ Pa}^{-1}$ as the calcination temperature changed from 1300 to 1500 °C. In comparison, Table 1 also shows the gas penetration coefficient of the sample made from 2 μm LSCF powder to be $1.69 \times 10^{-5} \text{ mL cm cm}^{-2} \text{ s}^{-1} \text{ Pa}^{-1}$ at 1200 °C. Since, the samples from the LSCF powder of 20 μm have better gas penetration coefficient even at higher sintering temperature than that of the sample from LSCF powder of 2 μm and PMMA beads of 5 μm

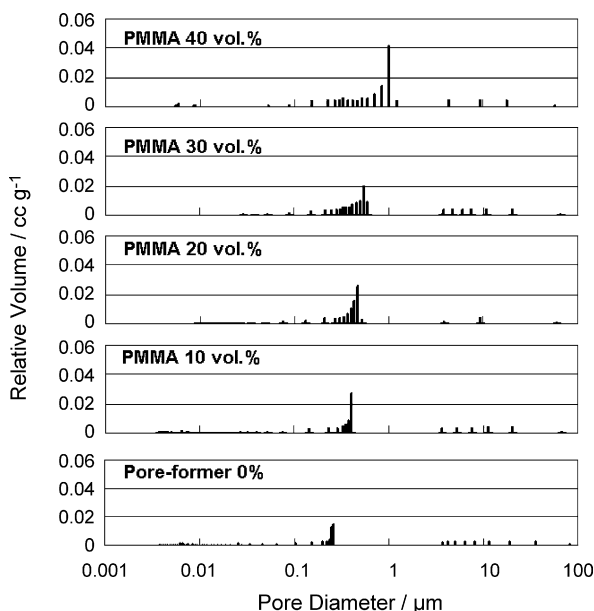


Fig. 6. Pore diameter distribution of the anode tubes with different PMMA addition.

Table 1
Gas penetration coefficient of the cathode matrix

Sample	Calcinations temperature (°C)	Gas penetration coefficient ($\text{mL cm cm}^{-2} \text{ s}^{-1} \text{ Pa}^{-1}$)
LSCF 20 μm	1300	1.68×10^{-4}
no pore-former	1400	1.41×10^{-4}
	1500	1.35×10^{-4}
LSCF 2 μm PMMA 40%	1200	1.69×10^{-5}

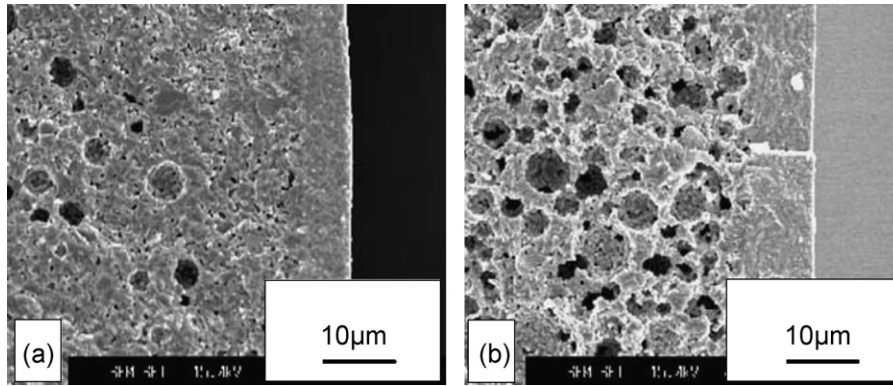


Fig. 7. SEM images of the cross-sections at the interface between the electrolyte and the anode tube: (a) PMMA 10 vol.%; (b) PMMA 40 vol.%.

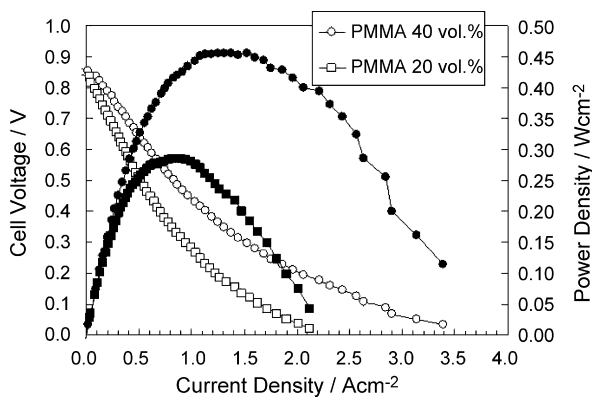


Fig. 8. The results of the power generation tests.

in diameter, use of large grains was chosen for the cathode matrices fabrication process.

Fig. 9 shows the relationship between estimated gas flow rate in the cathode matrices required to obtain volumetric power density of 2 W cm^{-3} (0.5 V , 4 A) and the gas penetration coef-

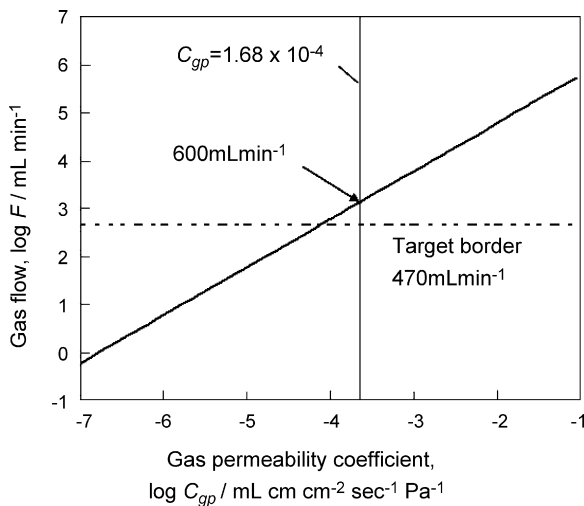


Fig. 9. Relationship between estimated gas flow rates in the cathode matrices required to obtain power density of 2 W cm^{-3} and the gas penetration coefficients of the cathode matrices under the pressure difference of 0.1 MPa between the inlet and outlet.

ficient of the cathode matrices under the pressure difference of 0.1 MPa between the inlet and outlet. The former gas flow rate was calculated with the amount of oxygen estimated from the current, the composition ratio of air and air utilization of 30% , which was typical value for standard SOFC operation [13]. The latter one was estimated with the pressure difference of 0.1 MPa and cubic cell size ($1 \text{ cm} \times 1 \text{ cm} \times 1 \text{ cm}$) by Eq. (1). Providing that the matrix has gas penetration coefficient of $1.68 \times 10^{-4} \text{ mL cm cm}^{-2} \text{ s}^{-1} \text{ Pa}^{-1}$, it is possible to flow 600 mL min^{-1} air in a cubic cell (1 cm^3) under 0.1 MPa difference between the inlet and outlet. The air flow of 470 mL min^{-1} is estimated from the target power density of 2 W cm^{-3} , the cathode matrices appeared to be suitable components for the cube to achieve targeted performance.

3.3. Assembly of cube shaped micro tubular SOFC bundles

The cube of $3 \text{ cm} \times 3 \text{ cm} \times 3 \text{ cm}$ was made by arranging 36 anode tubes in 6×6 configuration (2 mm diameter tubes). Fig. 10 shows the appearance of the cube using the prepara-

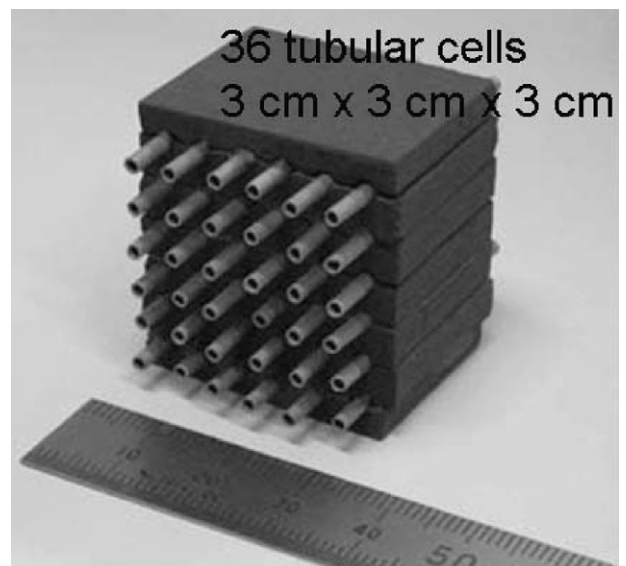


Fig. 10. The appearance of the cube.

tion method as shown in Fig. 3. As can be seen, the preparation method developed in this study was shown to be very effective for the fabrication of highly accumulated fuel cell bundles. The dimension of cubic cell bundle will be optimized by considering gas flow, current distribution, heat distribution, and so on. At the present stage, power characterization of the cube is under investigation.

4. Conclusion

The micro tubular cells whose diameters were 0.8 and 2.0 mm were successfully prepared using the preparation method developed in this study. It was shown that the anode structure could be controlled by changing the amount of the pore former (PMMA beads) without impairing the quality of electrolyte. The cathode matrices made from 20 μm LSCF grains show the best gas penetration coefficient of $1.68 \times 10^{-4} \text{ mL cm cm}^{-2} \text{ s}^{-1} \text{ Pa}^{-1}$, under 0.1 MPa difference between the inlet and outlet, which is sufficient for supplying enough gas to achieve targeted power output. These components were successfully assembled to be a cube shaped micro tubular SOFC bundles (3 cm \times 3 cm \times 3 cm) with 36 tubular cells (diameter of 2.0 mm). As future work, methods of gas sealing, and current collection, as well as the design of gas manifold for this cube will be investigated for micro tubular SOFC system.

Acknowledgement

This work had been supported by NEDO, as part of the Advanced Ceramic Reactor Project.

References

- [1] Y. Wang, C.-Y. Wang, *J. Power Sources* 147 (2005) 148–161.
- [2] I.H. Son, M. Shamsuzzoha, A.M. Lane, *J. Catal.* 210 (2002) 460–465.
- [3] K. Eguchi, H. Kojo, T. Takeguchi, R. Kikuchi, K. Sasaki, *Solid State Ionics* 152–153 (2002) 411–416.
- [4] Y. Mizutani, K. Hisada, K. Ukai, H. Sumi, M. Yokoyama, Y. Nakamura, O. Yamamoto, *J. Alloys Compd.* 408–412 (2006) 518–524.
- [5] D. Waldbillig, A. Wood, D.G. Ivey, *Solid State Ionics* 176 (2005) 847–859.
- [6] C. Hatchwell, N.M. Sammes, I.W.M. Brown, *Solid State Ionics* 126 (1999) 201–208.
- [7] J. Van herle, R. Ihringer, N.M. Sammes, G. Tompsett, K. Kendall, K. Yamada, C. Wen, T. Kawada, M. Ihara, J. Mizusaki, *Solid State Ionics* 132 (2000) 333–342.
- [8] M. Lockett, M.J.H. Simmons, K. Kendall, *J. Power Sources* 131 (2004) 243–246.
- [9] N.M. Sammes, Y. Du, R. Bove, *J. Power Sources* 145 (2005) 428–434.
- [10] B.C.H. Steel, *Solid State Ionics* 129 (2000) 95–110.
- [11] T. Otake, H. Yagami, K. Yashiro, Y. Nigara, T. Kawada, J. Mizusaki, *Solid State Ionics* 161 (2003) 181–186.
- [12] T. Hibino, A. Hashimoto, K. Asano, M. Yano, M. Suzuki, M. Sano, *Electrochem. Solid State Lett.* 5 (11) (2002) A242–A244.
- [13] B. Borglum, E. Tang, M. Pastula, J. Kessall, *Seventh European SOFC Forum*, 2006, p. B031.